966 Transaction of the Korean Society of Mechanical Engineers, Vol. 10, No. 6, pp. 966~975, 1986.

<Original>

Laminar Natural Convection in a Concentric Cylindrical Annulus with Wall Conductivity Effect

Seong-Keun Park* and Keun-Shik Chang**

(Received June 12, 1986)

有限 熱傳導率을 갖는 水平同心圓管 사이에서의 層流自然對流

박 성 근·장 근 식

Key Words: Natural Convection(自然對流), Concentric Cylinder(同心圓管), Wall Conductivity(管 熱傳導率), Finite Difference Method(有限次分法), Equivalent Conductivity(等價熱傳導係數)

초 록

有限한 熱傳導率과 두께를 갖는 水平同心圓管 內의 層流自然對流 문제를 有限次分法을 사용하여 數値的으로 硏究하였다. 同心圓管 內에는 傳導—對流가 復合되어, 團體—流體 境界面에서의 溫度分布는 미리 알려져 있지 않다. Prandtl 數를 0.7, $L/D_i=0.8$로 고정하고 각각의 Rayleigh 數와 熱傳導係數의 比, 幾何學的變數에 대하여 계산을 수행하였으며, 그 결과를 等溫 水平同心圓管의 경우와 비교하였다. Rayleigh 數와 t/D_i가 클수록, 熱傳導係數의 比 K가 작을수록 熱傳導 效果는 강하게 나타났으며, 局所等價傳導係數와 溫度分布에 비하여 速度分布는 영향을 덜 받는다는 것이 밝혀졌다.

Nomenclature

B : Dummy variable

D_i : Inner cylinder diameter ($=2R_1$)

k : Thermal conductivity

K : Wall to fluid conductivity ratio, k_w/k_f

K_{eq} : Local equivalent conductivity, $r\frac{\partial\phi}{\partial r}\Big)_r \cdot \{\ln(r_1/r_0)/K+\ln(r_2/r_1)+\ln(r_3/r_2)/K\}$

$\overline{K}_{eq}$: Average equivalent conductivity, $\frac{1}{\pi}\int_0^{\pi} K_{eq}d\theta$

L : Gap width (characteristic length)

Pr : Prandtl number, ν/α

Ra : Rayleigh number based on gap width, $g\beta L^3(T_i-T_0)/\nu\alpha$

r, θ : Dimensionless cylindrical coordinates

R : Dimensional cylindrical radial coordinates

t : Cylinder wall thickness (for both of the inner and outer wall)

T_i, T_0 : Inner surface temperature of the inner wall and outer surface temperature of the outer wall

* Dept. of Mech. Eng., KAIST

** Member, Dept. of Mech. Eng., KAIST

V_{max} : Maximum angular velocity in the convection region
α : Thermal diffusivity
ν : Kinematic viscosity
ϕ : Dimensionless temperature
ψ : Dimensionless streamfunction
ω : Dimensionless vorticity

Subscript

w : Interface wall
f : Fluid

1. Introduction

Laminar natural convection heat transfer in a variety of enclosures has been of much interest in the practical view point for many years. In particular, the horizontal concentric annulus has attracted great attention because of its many engineering applications. Examples are the solar collectors, nuclear reactor design[1], aircraft cabin insulation[2], pressurized-gas underground electric transmission cable[3] and so on.

After the first study of Beckmann[4], many authors participated in the research of the concentric circular annulus problems. Powe, Carley & Bishop[5] showed qualitative flow patterns of air using smoke visualization technique; Eckert & Soehngen[6] and Hauf & Grigull[7] obtained local heat transfer coefficients using Mach-Zehnder interferometer. The first numerical study was made by Crawford & Lemlich[8] with Gauss-Seidel iterative method. Kuehn & Goldstein[9] offered an extensive review of previous experimental and theoretical works, while they themselves used Mach-Zehnder interferometer to measure the local and average equivalent heat conductivities. Rayleigh number ranges considered were from 2.11×10^4 to 9.16×10^5 for the air and water, with the gap to diameter ratio 0.8. They also made the numerical calculations using the successive over-relaxation method. Recently, extention of the research was made by Farouk & Guceri[10] to turbulent regime using the two-equation turbulence modeling, and by Cho, Chang & Park[11] to eccentric annulus by using the bipolar coordinates.

All the studies mentioned above assumed, however, infinite conductivity and uniform temperature boundary conditions, while most of the physical boundaries have, strictly speaking, finite conductivities and non-uniform temperature distributions. Rotem[12] studied the free convection in interaction with a heat dissipating and conducting core by expanding the perturbation series of streamfunction and temperature with the Grashof number and the Rayleigh number, respectively. In the recent report by Burch et al.[13], laminar natural convection flow between vertical plates with finite conduction rate was studied by using boundary layer approximation. They used Partankar-Spalding type finite difference scheme to obtain the temperature field, heat flux distribution at the solid-fluid interface and velocity profiles in the boundary layer regions. The results were compared with the case of infinite conductivity. D.M. Kim & R. Viskanta[14] reported about free convective flows in a square enclosure with non-uniform boundary temperature distributions, and Chung et al.[15] studied the effect of conductivity and thickness on natural convection heat transfer from a horizontal circular tube.

The purpose of this paper is to include the wall conduction effect for a free convective flow in an horizontal concentric annulus, which has been so far treated with constant temperature boundary conditions only. This extension of the classical concentric annulus problem will enable engineers to obtain more realistic data useful for the practical situations. In this study

numerical solution is obtained for the coupled conduction-convection governing equations with the constant thermodynamic property assumptions. The thermal conditions along the solid-fluid interface are not known a priori to the calculations, but can be determined iteratively through coupling of the natural convection and the two-dimensional wall conduction during the calculations.

2. Mathematical Formulation

Steady two dimensional incompressible laminar fow is assumed. The Boussinesq approximation of constant fluid properties except for the buoyancy force term is supposed to hold. Due to the vertical symmetry of the problem, only half of the flow domain is considered. The thermal conditions at the solid-fluid interfaces are not known a priori.

The governing equations are formulated in cylindrical polar coordinates, where the coordinates are R, measured from the center of the system, and θ, measured clockwise from the upward vertical line. The radial velocity, defined by $U=R^{-1}\partial\Psi/\partial\theta$ is positive radially outward, the angular velocity, defined by $V=-\partial\Psi/\partial R$ is positive in the clockwise direction for $0°<\theta<180°$. In order to nondimensionalize the equation, the following dimensionless variables are used

$$\psi=\Psi/\alpha,\ r=R/L,\ \phi=\frac{T-T_0}{T_i-T_0},$$

$$u=\frac{UL}{\alpha},\ v=\frac{VL}{\alpha}$$

where $\alpha=k/\rho c$ is the thermal diffusivity, L is the gap width between the cylinders T_i is the temperature of the inner surface of the inner cylinder wall and T_0 is that of the outer surface of the outer cylinder wall. By introducing the vorticity ω, the governing equations become

$$\nabla^2\psi=-\omega \tag{1}$$

$$\nabla^2\omega=\frac{1}{Pr}\left[u\frac{\partial\omega}{\partial r}+\frac{v}{r}\frac{\partial\omega}{\partial\theta}\right]+Ra\left[\sin\theta\frac{\partial\phi}{\partial r}+\frac{\cos\theta}{r}\cdot\frac{\partial\phi}{\partial\theta}\right] \tag{2}$$

$$\nabla^2\phi=u\frac{\partial\phi}{\partial r}+\frac{v}{r}\frac{\partial\phi}{\partial\theta} \tag{3}$$

in the convection region and

$$\nabla^2\phi=0 \tag{4}$$

in the inner and outer conducting wall (see Fig. 1).

The parameters appearing in the problem are Rayleigh number Ra, Prandtl number Pr, the wall to fluid conductivity ratio $K(=k_w/k_f)$, and the geometric parameters. The last includes the gap to inner diameter ratio L/D_i, and the conducting wall thickness to inner cylnder daimeter ratio t/D_i. Detailed geometry configuration is presented in Fig. 1.

The boundary conditions imposed on this problem are

$$\psi=u=v=0,\ \omega=-\frac{\partial^2\psi}{\partial r^2}$$

$$\text{at } r=r_2 \text{ and } r=r_1 \tag{5}$$

and on the symmetry lines

$$\psi=\frac{\partial u}{\partial\theta}=v=\omega=\frac{\partial\phi}{\partial\theta}=0 \tag{6}$$

and the temperature Dirichlet conditions

$$\phi=0 \text{ at } r=r_3 \tag{7}$$

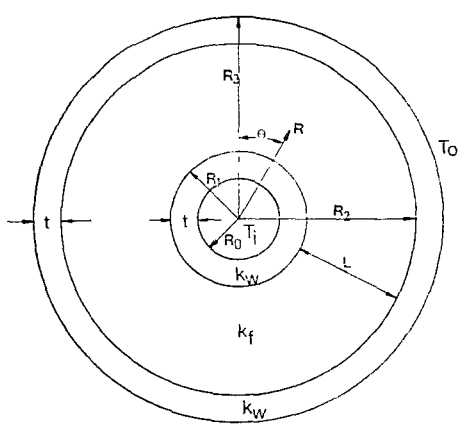

Fig. 1 Problem configuration

$$\phi=1 \text{ at } r=r_0 \tag{8}$$

The thermal conditions at the solid-fluid interfaces are not known until the problem is solved. However, we can determine these conditions iteratively as the numerical solution converges, by imposing the continuity requirement for the temperature and the heat flux at the solid-fluid interfaces as

$$\phi_w=\phi_f \text{ at } r=r_2 \text{ and } r=r_1 \tag{9}$$

$$K\frac{\partial\phi}{\partial r}\Big)_w=\frac{\partial\phi}{\partial r}\Big)_f \text{ at } r=r_2 \text{ and } r=r_1 \tag{10}$$

3. Solution Methodology

The finite difference approach is used in the present problem to obtain solutions at the discrete grid points. The central difference schemes are adopted for the interior node points, while at the boundary node points one-sided difference formulations of first order accuracy are employed. The ADI(Alternating Direction Implicit)[14] schemes are used for the transport equations (i.e. the vorticity equation and the energy equation) and SOR (Successive Over Relaxation) methods are used for the rest of the equations.

The employment of the grid points are carefully monitored to ensure grid-independent results. Grid stretching is made in the radial as well as in the azimuthal directions by combining appropriate trigonometric functions. Near the upper symmetry line $\theta=0°$ and near the solid-fluid interfaces where large gradients are expected, grid points are concentrated. In the conducting wall regions, uniform mesh is used in the r-direction and the same mesh size is used in the θ-direction as in the convective region. The total number of grid points employed in the computation is 21×25 in r and θ-direction, respectively, in the convective region and 7×25 grid points in both of the conducting wall regions. The accuracy of the present numerical procedure is verified by comparing the solutions obtained for the case of uniform wall temperature with the results of Kuehn & Goldstein[9].

As noted earlier, to determine the temperature and heat flux at the solid-fluid interfaces, cyclic interation is performed to get the solution satisfying the governing equations and boundary conditions. The procedure is initiated by assuming plausible temperature profiles at the solid-fluid interfaces. The natural convection equations are then solved based on the assumed temperature boundary condition. The heat flux distribution obtained from this solution is then used as one of the boundary conditions for the wall conduction equation. The solution of this conduction equation yields a new interface temperature profiles, which are used again as the new boundary values for the temperature in the natural convection region. These processes form a cyclic iteration by which the convection and conduction regions numerically converge towards a steady state.

The solution is considered to be converged when each of the streamfunction, vorticity and temperature variables meets the following criterion.

$$\|(B^{n+1}-B^n)/B^n\|<10^{-3} \tag{11}$$

where the superscript n denotes an iteration index and $\|\cdot\|$ themaximum norm.

4. Result and Discussion

The present problem deals with the effect of finite wall conductivity in a concentric annulus filled with air. The outer surface of the outer wall is maintained at a uniform dimensionless temperature $\phi=0$ and the inner surface of the inner wall at $\phi=1$. Since finite conductivity is assumed, the thermal conditions along the

solid-fluid interface are not known a priori. For simplicity of the problem the inner and outer wall thickness and conductivity are assumed same for both of the conducting walls. The results are obtained for the gap to diameter ratio $L/D_i=0.8$ and Rayleigh numbers $Ra=10^3$, 10^4 and 5×10^4. These allow us to compare the results directly with the previously published data of Kuehn and Goldstein[9]. In order to study the effect of the wall thermal resistance, calculations performed for the wall thickness to diameter $t/D_i=0.1$ and 0.2, and the wall to fluid conductivity ratio $K=1$, 10 and 100. Especially $K=10^6$ is substituted for $K=\infty$ condition, and maximum temperature nonuniformity due to it is less than only 0.001%. For very small K, the solution converges very slowly and moreover for $K\to0$ (adiabatic) the problem becomes ill-conditioned.

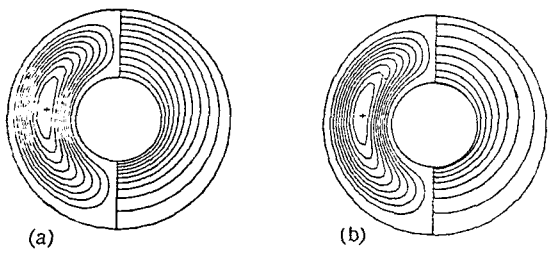

(a) uniform wall temperatures: $\Delta\psi=0.23$, $\Delta\phi=0.1$
(b) conducting walls: $K=1$, $t/D_i=0.1$, $\Delta\psi=0.17$, $\Delta\phi=0.1$

Fig. 2 Isotherms andstreamline contours at $Ra=10^3$

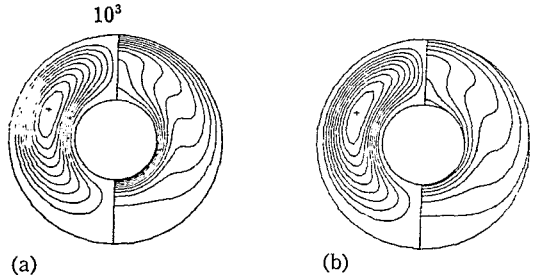

(a) uniform wall temperatures: $\Delta\psi=1.32$, $\Delta\phi=0.1$
(b) conducting walls: $K=1$, $t/D_i=0.1$, $\Delta\psi=0.93$, $\Delta\phi=0.1$

Fig. 3 Isotherms and streamline contours at $Ra=10^4$

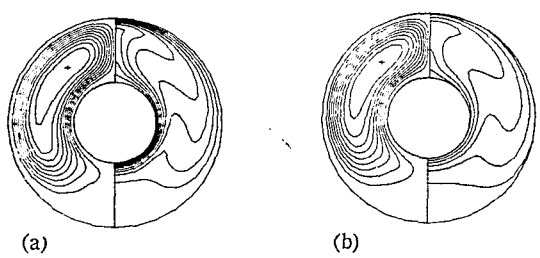

(a) uniform wall temperatures: $\Delta\psi=2.47$, $\Delta\phi=0.1$
(b) conducting walls: $K=1$, $t/D_i=0.1$, $\Delta\psi=1.65$, $\Delta\phi=0.1$

Fig. 4 Isotherms and streamline contours at $Ra=5\times10^4$

4.1 The Isotherms and Streamlines

Each Figs. 2(b), 3(b), 4(b) shows the streamlines and isotherms for different Rayleigh numbers $Ra=10^3$, 10^4, 5×10^4, respectively, for fixed parameters $Pr=0.7$, $L/D_i=0.8$, $K=1$ and $t/D_i=0.1$. In the Figs. 2(a), 3(a), 4(a) juxtaposed are the results of the constant wall temperature problems. The isotherms in the right hand side figures emerge from the inner boundary and are terminated at the outer boundary. The wall heat conduction effect reduces the average temperature difference across the gap, the buoyancy induced flow in the annulus is weaker than that of the uniform temperature problem. But both of the flow patterns are qualitatively very similar despite the different strength of the recirculating stream.

4.2 Interface Temperatures

Figs. 5~7 present the temperature distributions along the solid-fluid interfaces for Rayleigh numbers, $Ra=10^3$, 10^4 and 5×10^4, respectively. The buoyancy force lifts the warmer fluid upward, which generates the fluid convection and causes a non-uniform heat flux along the interfaces. The curves show that temperature at the upper parts of the inner

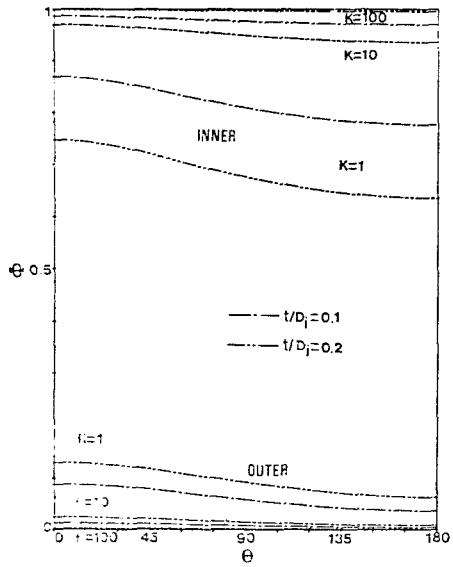

Fig. 5 Interface temperature distribution at $Ra=10^3$

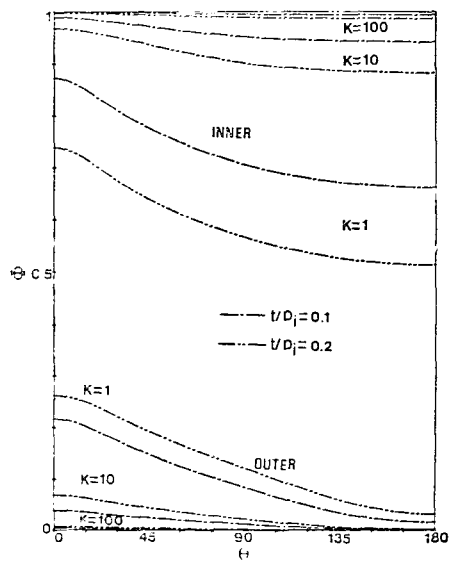

Fig. 6 Interface temperature distribution at $Ra=10^4$

and outer cylinder is higher. The upward boundary layer flow of the inner cylinder started from the bottom is heated while it passes along the inner cylinder surface. It gives the highest temperature and so the least heat flux at the top. The boundary layer flow shedded from

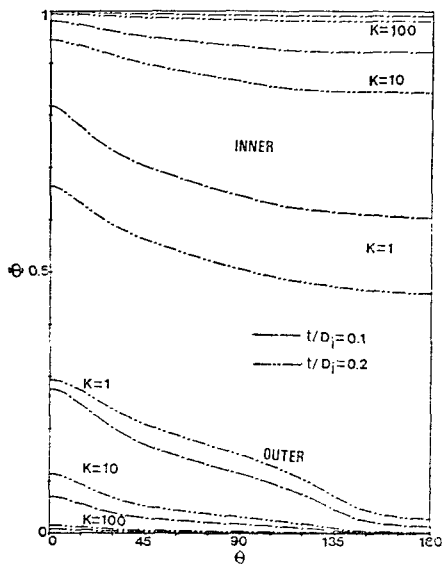

Fig. 7 Interface temperature distribution at $Ra=5\times10^4$

the inner cylinder forms a hot rising plume which impinges on the top of the outer cylinder interface. This makes the upper part of the outer cylinder hot and of the highest heat flux. The downward boundary layer near the outer cylinder interface gets cooled as it moves downward. So, it has the least heat flux and the lowest temperature at the bottom. If conductivity of the solid wall is assumed to be infinite, transmitted heat to the interface will be removed or supplied with infinite rate and so uniform temperature can be set up. In reality all the material have finite conductivity and thus the finite conduction rate. It makes interfacial temperature more or less non-uniform. In overall, the outer cylinder becomes warmer due to the impinging plume and the inner one becomes cooler due to convective cooling than those of the uniform temperature problem.

It may be observed from Figs. 5~7 that for each Rayleigh number, decreasing K or increasing t/D_i tends to lower the inner interface

temperature and to raise the outer interface temperature. The smaller K and the larger t/D_i result in a larger temperature drop across the solid wall and therefore smaller tempe rature difference between the interfaces. These conditions also contribute to the interface temperature profiles more non-uniform. It is due to the increased thermal resistances of the wall. The influence of wall conduction appears increasingly more pronounced with higher Rayleigh numbers. As the Rayleigh number increases, the equivalent conductivity K_{eq} also increases. This may be understood as the lowering effect of the wall to fluid conductivity ratio K. For example, at $Ra=10^3$, $t/D_i=0.1$ and $K=100$ the maximum deviation from the uniform interface temperature is less than 0.5% only, but at $Ra=5\times10^4$, $t/D_i=0.1$ and $K=100$ the maximum deviation is more than 1%. Furthermore, in view of the non-uniform interface temperature distribution the conduction in the solid wall is clearly two dimensional. Therefore two dimensional conduction equation should be solved even though the geometry is axisymmetric. Only if the conductivity ratio is sufficiently large and the wall thickness ratio is sufficiently small, the interface temperature can be safely assumed to be uniform in the moderate error bounds.

4.3 Interface Heat Fluxes

Generally in natural convection heat transfer within an enclosure the heat flux is expressed by means of the dimensionless parameter K_{eq} which is called the local equivalent conductivity. It is defined as a ratio of the local convective heat flux to the pure conduction heat flux.

The local equivalent conductivity distributions are presented in Figs. 8~11 for Rayleigh numbers $Ra=10^4$ and 5×10^4, and $t/D_i=0.1$ and 0.2. The heat flux distribution for the uniform temperature case is also shown in each figure by solid lines. These solid lines agree very well to the data of Kuehn and Goldstein[9]. For each Rayleigh numbers, at

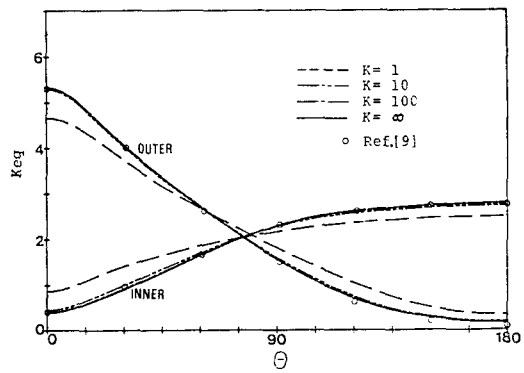

Fig. 8 Local equivalent conductivity distribution at $Ra=10^4$ and $t/D_i=0.1$

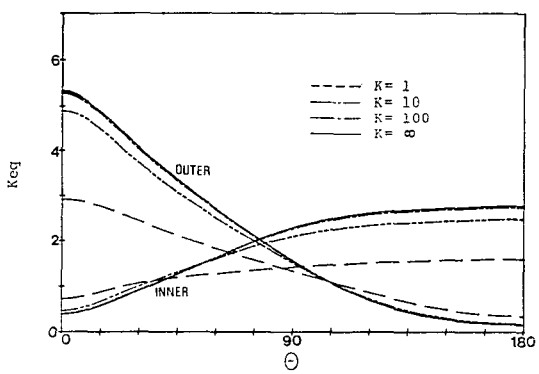

Fig. 9 Local equivalent conductivity distribution at $Ra=10^4$ and $t/D_i=0.2$

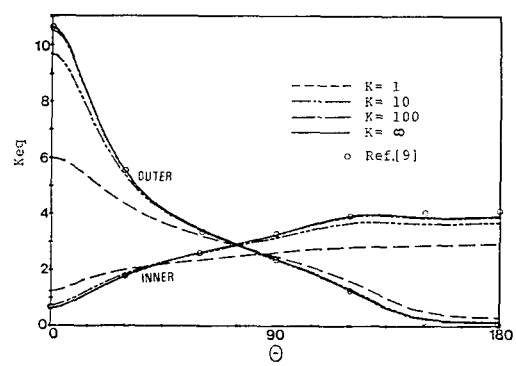

Fig. 10 Local equivalent conductivity distribution at $Ra=5\times10^4$ and $t/D_i=0.1$

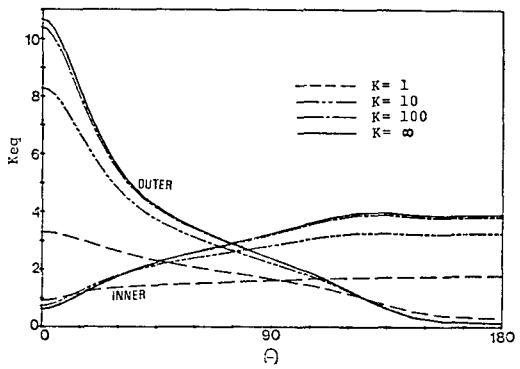

Fig. 11 Local equivalent conductivity distribution at $Ra=5\times10^4$ and $t/D_i=0.2$

larger K and smaller t/D_i values these plots approach more to the solid lines as expected. In contrast to the wall temperature plots in Figs. 5~7, the maximum deviation of the local heat flux from that of the uniform wall temperature case is less pronounced. For example, in Fig. 6 the maximum temperature deviation from the uniform wall temperature case is about 1% for $K=100$ and $t/D_i=0.1$; for the same parameters, however, the maximum heat flux deviation is less than 0.5%. The average equivalent conductivity $\overline{K}_{eq}$ also decreases, as K decreases and t/D_i increases. It is because the large thermal resistance lowers the temperature difference in the annulus and thus the effective Rayleigh number, which can be defined from the temperature difference between the interfaces. The influence of the conductivity ratio K on the heat flux distribution is more significant at high Rayleigh numbers. It is because for high Rayleigh numbers the large value of the average equivalent conductivity $\overline{K}_{eq}$ plays the role of lowering the conductivity ratio K.

For the average equivalent conductivity $\overline{K}_{eq}$, a correlation similar to Chung et al.[15] can be derived. The computed average equivalent conductivity is almost proportional to both of exp $(-A\cdot K)$ and t/D_i, where A is a constant. Fitting the computed results to one-fourth power law gives for air

$$\overline{K}_{eq}=Ra^{0.25}\{0.195-0.1595\exp(-0.0253K)(t/D_i)\} \quad (12)$$

where $10^4<Ra<5\times10^4$, $1<K<100$, $0.1<t/D_i<0.2$. The maximum discrepancy of the computed $\overline{K}_{eq}$ to this correlation is less than 2%.

4.4 Velocity Profiles

The angular velocity profiles along the radial lines at $\theta=45°$, 90° and 135° are plotted in Figs. 12~15 for $Ra=10^4$ and 5×10^4, and for $t/D_i=0.1$ and 0.2. These angular velocities are scaled by their maximum values. As it can be seen from Figs. 12~15, the scaled velocity profiles are similar to each other. From Figs. 2~4 it was already expected, of course. In

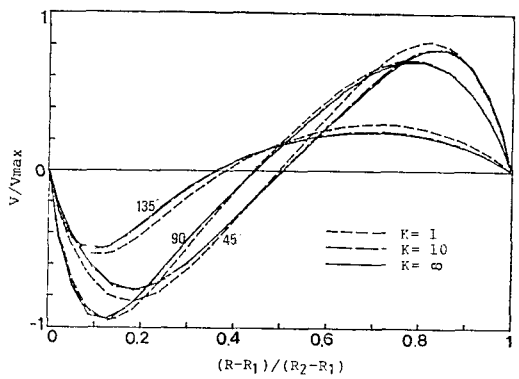

Fig. 12 Normalized angular velocity distribution at $Ra=10^4$ and $t/D_i=0.1$

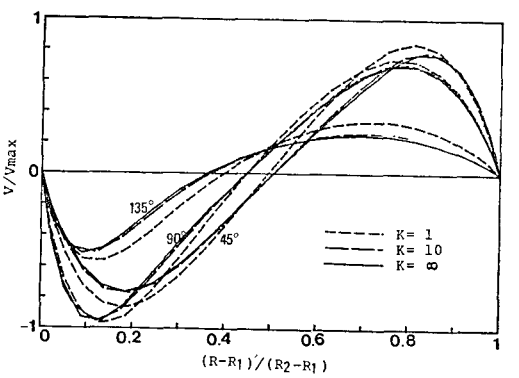

Fig. 13 Normalized angular velocity distribution at $Ra=10^4$ and $t/D_i=0.2$

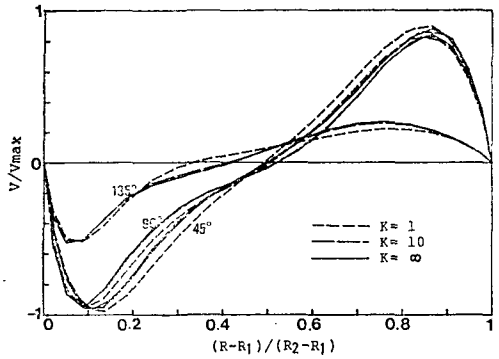

Fig. 14 Normalized angular velocity distribution at $Ra=5\times10^4$ and $t/D_i=0.1$

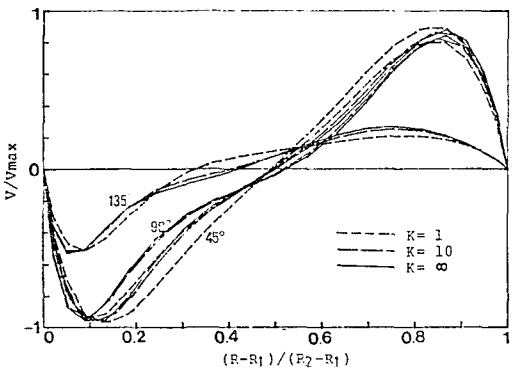

Fig. 15 Normalized angular velocity distribution at Ra$=5\times10^4$ and $t/D_i=0.2$

spite of different leveling of the streamline contours at given Rayleigh numbers, the shapes of the streamline contours resemble each other. For example, at $Ra=5\times10^4$ the ratio of the maximum velocity of the conducting wall ($K=1$, $t/D_i=0.1$) to that of the uniform temperature wall is about 67%; the scaled velocity profiles have the maximum discrepancy of about 10%only. Furthermore, for $K=10$ and $t/D_i=0.1$ the scaled velocity profile discrepancy is less than about 1%, and the maximum velocity agrees upto about 95%. It implies that the velocity profile is considerably less sensitive to the influence of the finite wall conductivity. If a material of low conductivity such as glass, is used for the hypothetical constant temperature wall for flow visualization purpose, the observed velocity profiles would give relatively satisfactory data. Comparison of the curves in Figs. 12~15 reveals that the wall thickness effect causes less influence to the velocity profiles than to the temperature profiles and the heat flux distribution along the interfaces.

5. Conclusions

Results of a numerical study of laminar natural convection coupled with the wall conduction effect in a concentric cylindrical annulus have been presented. Outputs obtained are the temperature and local equivalent conductivity distribution along the solid-fluid interfaces and the velocity profiles in the annulus. The entire results were compared with case of the wall with infinite conductivity. Results indicate that the conduction causes significant influence on the natural convection heat transfer, particulary at high Rayleigh numbers, low K and high t/D_i. The difference between the case of the uniform wall temperature and that of the wall of finite conductivity is smaller for high K and low t/D_i values, at each fixed Rayleigh number. For very high K and low t/D_i values, the results agreed very well with the already published data of Kuehn and Goldstein.[9] When the azimuthal velocity component is normalized with its maximum value, the velocity profiles for the wall of finite conductivity and the uniform temperature wall agreed fairly well to each other. It implies that the velocity profiles are less sensitive to the influence of the finite conductivity.

References

(1) K.L. Peddicord, B.D. Ganapol, & R. Henninger, A Consistent Algorithm for the Study of Heat Transfer in Eccentric Annuli, American Nuclear

Society Transactions, Vol. 22, pp. 572~573, 1975

(2) M.R. Abbort, A Numerical Method for Solving the Equations of Natural Convection in a Narrow Concentric Cylindrical Annulus with a Horizontal Axis, Qurtery Journal of Mechanics and Applied Mathematics, Vol. 17, pp. 471~481, 1964

(3) B.O. Pedersen, H.C. Doepken & P.C. Bolin, Development of a Compressed Gas Insulated Transmission Line, IEEE Winter Power Meeting, paper 71 TP 193-PWR, 1971

(4) W. Beckmann, Die Wärmeübertragung in Zylindrischen Gasschichten bei natürlicher Konvektion, Forsch. Geb. d. Ingenierurwesen, 2[5], pp. 165~178, 1931

(5) R.E. Pow, C.T. Carley & E.H. Bishop, Free Convective Flow Patterns in Cylindrical Annuli, ASME J. of Heat Transfer, Vol. 91, pp. 310~314, 1969

(6) E.R.G. Eckert & E.E. Soehgen, Studies on Heat Transfer in Laminar Free Convection with Zehnder-Mach Interferometer, Wright-Patterson AFB Tech. Rep. No. 5747, ATI-44580, 1948

(7) U. Grigull & W. Hauf, Natural Convection in Horizontal Cylindrical Annuli, 3rd Int. Heat. Transfer Conf., Chicago, pp. 182~185, 1966

(8) L. Crawford & R. Lemlich, Natural Convection in Horizontal Concentric Cylindrical Annuli, I.E.C. Fund, 1, pp. 260~264, 1962

(9) T.H. Kuehn & R.J. Goldstein, An Experimental and Theoretical Study of Natural Convection in the Annulus between Horizontal Concentric Cylinders, J. of Fluid Mech., Vol. 74, part 4, pp. 695~719, 1976

(10) B. Farouk & S.I. Guceri, Laminar and Turbulent Natural Convection in the Annulus between Horizontal Concentric Cylinders, ASME J. of Heat Transfer, Vol. 104, pp. 631~636, 1982

(11) C.H. Cho, K.S. Chang & K.H. Park, Numerical Simulation of Natural Convection in Concentric and Eccentric Horizontal Cylindrical Annuli, ASME J. of Heat Transfer, Vol. 104, pp. 624~630, 1982

(12) Z. Rotem, Conjugate Free Convection from Horizontal Conducting Circular Cylinders, Int. J. of Heat and Mass Transfer, Vol. 15, pp. 1679~1693, 1972

(13) T. Burch, T. Rhodes & S. Acharya, Laminar Natural Convection between Finitely Conducting-Vertical plates, Int. J. of Heat and MassTransfer, Vol. 28, No. 6, pp. 1173~1186, 1985

(14) D.M. Kim & R. Viskanta, Effect of Wall Heat Conduction on Natural Convection Heat Transfer in a Square Enclosure, ASME J. of Heat Transfer, Vol. 107, pp. 139~146, 1985

(15) H.S. Chung, B.H. Kang & S.S. Kwon, Effect of Conductivity and Thickness on Natural Convection Heat Transfer from a Horizontal Circular Tube, KSME, Vol. 10, No. 2, pp. 265~279, 1986